

World Journal of *Gastrointestinal Oncology*

World J Gastrointest Oncol 2021 December 15; 13(12): 1850-2222



FRONTIER

- 1850 Management of obstructive colon cancer: Current status, obstacles, and future directions
Yoo RN, Cho HM, Kye BH

REVIEW

- 1863 Role of endoscopic ultrasound in anticancer therapy: Current evidence and future perspectives
Bratanic A, Bozic D, Mestrovic A, Martinovic D, Kumric M, Ticinovic Kurir T, Bozic J
- 1880 Pancreatic intraductal papillary mucinous neoplasms: Current diagnosis and management
Jabłońska B, Szmigiel P, Mrowiec S
- 1896 Combined treatments in hepatocellular carcinoma: Time to put them in the guidelines?
Sparchez Z, Radu P, Bartos A, Nenu I, Craciun R, Mocan T, Horhat A, Spârchez M, Dufour JF
- 1919 Unique situation of hepatocellular carcinoma in Egypt: A review of epidemiology and control measures
Ezzat R, Eltabbakh M, El Kassas M
- 1939 Moving forward in the treatment of cholangiocarcinoma
Manzia TM, Parente A, Lenci I, Sensi B, Milana M, Gazia C, Signorello A, Angelico R, Grassi G, Tisone G, Baiocchi L
- 1956 Solid extraintestinal malignancies in patients with inflammatory bowel disease
Mala A, Foteinogiannopoulou K, Koutroubakis IE
- 1981 Mesenchymal stem cell-derived exosomes for gastrointestinal cancer
Zhao LX, Zhang K, Shen BB, Li JN
- 1997 Diabetes mellitus contribution to the remodeling of the tumor microenvironment in gastric cancer
Rojas A, Lindner C, Schneider I, González I, Araya H, Morales E, Gómez M, Urdaneta N, Araya P, Morales MA
- 2013 Macrophages play a role in inflammatory transformation of colorectal cancer
Lu L, Liu YJ, Cheng PQ, Hu D, Xu HC, Ji G

MINIREVIEWS

- 2029 Advancement of chimeric antigen receptor-natural killer cells targeting hepatocellular carcinoma
Dai K, Wu Y, She S, Zhang Q
- 2038 Current status of first-line therapy, anti-angiogenic therapy and its combinations of other agents for unresectable hepatocellular carcinoma
Alqahtani SA, Colombo MG

- 2050** Endoscopic or percutaneous biliary drainage in hilar cholangiocarcinoma: When and how?
Mocan T, Horhat A, Mois E, Graur F, Tefas C, Craciun R, Nenu I, Spârchez M, Sparchez Z
- 2064** Current status of non-surgical treatment of locally advanced pancreatic cancer
Spiliopoulos S, Zurlo MT, Casella A, Laera L, Surico G, Surgo A, Fiorentino A, de'Angelis N, Calbi R, Memeo R, Inchingolo R
- 2076** Prospect of lenvatinib for unresectable hepatocellular carcinoma in the new era of systemic chemotherapy
Sho T, Morikawa K, Kubo A, Tokuchi Y, Kitagataya T, Yamada R, Shigesawa T, Kimura M, Nakai M, Suda G, Natsuizaka M, Ogawa K, Sakamoto N

ORIGINAL ARTICLE**Basic Study**

- 2088** Dysbiosis of the duodenal microbiota as a diagnostic marker for pancreaticobiliary cancer
Sugimoto M, Abe K, Takagi T, Suzuki R, Konno N, Asama H, Sato Y, Irie H, Watanabe K, Nakamura J, Kikuchi H, Takasumi M, Hashimoto M, Kato T, Kobashi R, Hikichi T, Ohira H
- 2101** MutL homolog 1 methylation and microsatellite instability in sporadic colorectal tumors among Filipinos
Cabral LKD, Mapua CA, Natividad FF, Sukowati CHC, Cortez ER, Enriquez MLD
- 2114** Propofol induces ferroptosis and inhibits malignant phenotypes of gastric cancer cells by regulating miR-125b-5p/STAT3 axis
Liu YP, Qiu ZZ, Li XH, Li EY
- 2129** BRAF^{V600E} mutant colorectal cancer cells mediate local immunosuppressive microenvironment through exosomal long noncoding RNAs
Zhi J, Jia XJ, Yan J, Wang HC, Feng B, Xing HY, Jia YT

Retrospective Cohort Study

- 2149** Hepatocellular carcinoma surveillance and quantile regression for determinants of underutilisation in at-risk Australian patients
Low ES, Apostolov R, Wong D, Lin S, Kutaiba N, Grace JA, Sinclair M
- 2161** Comparison of tumor regression grading systems for locally advanced gastric adenocarcinoma after neoadjuvant chemotherapy
Liu ZN, Wang YK, Zhang L, Jia YN, Fei S, Ying XJ, Zhang Y, Li SX, Sun Y, Li ZY, Ji JF

Retrospective Study

- 2180** Clinical features of intracerebral hemorrhage in patients with colorectal cancer and its underlying pathogenesis
Deng XH, Li J, Chen SJ, Xie YJ, Zhang J, Cen GY, Song YT, Liang ZJ

Prospective Study

- 2190** Anatomic resection improved the long-term outcome of hepatocellular carcinoma patients with microvascular invasion: A prospective cohort study
Zhou JM, Zhou CY, Chen XP, Zhang ZW

SYSTEMATIC REVIEWS

- 2203** Minimally invasive surgical treatment of intrahepatic cholangiocarcinoma: A systematic review
Patrone R, Izzo F, Palaia R, Granata V, Nasti G, Ottaiano A, Pasta G, Belli A

LETTER TO THE EDITOR

- 2216** Gender differences in the relationship between alcohol consumption and gastric cancer risk are uncertain and not well-delineated
Verma HK, Bhaskar L
- 2219** Critical biomarkers of hepatocellular carcinoma in body fluids and gut microbiota
Nath LR, Murali M, Nair B

ABOUT COVER

Editorial Board Member of *World Journal of Gastrointestinal Oncology*, Ladan Teimoori-Toolabi, MD, PhD, Associate Professor, Department of Molecular Medicine, Pasteur Institute of Iran, Tehran 1316943551, Iran.
iteimoori@pasteur.ac.ir

AIMS AND SCOPE

The primary aim of *World Journal of Gastrointestinal Oncology (WJGO, World J Gastrointest Oncol)* is to provide scholars and readers from various fields of gastrointestinal oncology with a platform to publish high-quality basic and clinical research articles and communicate their research findings online.

WJGO mainly publishes articles reporting research results and findings obtained in the field of gastrointestinal oncology and covering a wide range of topics including liver cell adenoma, gastric neoplasms, appendiceal neoplasms, biliary tract neoplasms, hepatocellular carcinoma, pancreatic carcinoma, cecal neoplasms, colonic neoplasms, colorectal neoplasms, duodenal neoplasms, esophageal neoplasms, gallbladder neoplasms, *etc.*

INDEXING/ABSTRACTING

The *WJGO* is now indexed in Science Citation Index Expanded (also known as SciSearch®), PubMed, PubMed Central, and Scopus. The 2021 edition of Journal Citation Reports® cites the 2020 impact factor (IF) for *WJGO* as 3.393; IF without journal self cites: 3.333; 5-year IF: 3.519; Journal Citation Indicator: 0.5; Ranking: 163 among 242 journals in oncology; Quartile category: Q3; Ranking: 60 among 92 journals in gastroenterology and hepatology; and Quartile category: Q3. The *WJGO*'s CiteScore for 2020 is 3.3 and Scopus CiteScore rank 2020: Gastroenterology is 70/136.

RESPONSIBLE EDITORS FOR THIS ISSUE

Production Editor: *Ying-Yi Yuan*; Production Department Director: *Xiang Li*; Editorial Office Director: *Ya-Juan Ma*.

NAME OF JOURNAL

World Journal of Gastrointestinal Oncology

ISSN

ISSN 1948-5204 (online)

LAUNCH DATE

February 15, 2009

FREQUENCY

Monthly

EDITORS-IN-CHIEF

Rosa M Jimenez Rodriguez, Pashtoon M Kasi, Monjur Ahmed, Florin Burada

EDITORIAL BOARD MEMBERS

<https://www.wjgnet.com/1948-5204/editorialboard.htm>

PUBLICATION DATE

December 15, 2021

COPYRIGHT

© 2021 Baishideng Publishing Group Inc

INSTRUCTIONS TO AUTHORS

<https://www.wjgnet.com/bpg/gerinfo/204>

GUIDELINES FOR ETHICS DOCUMENTS

<https://www.wjgnet.com/bpg/GerInfo/287>

GUIDELINES FOR NON-NATIVE SPEAKERS OF ENGLISH

<https://www.wjgnet.com/bpg/gerinfo/240>

PUBLICATION ETHICS

<https://www.wjgnet.com/bpg/GerInfo/288>

PUBLICATION MISCONDUCT

<https://www.wjgnet.com/bpg/gerinfo/208>

ARTICLE PROCESSING CHARGE

<https://www.wjgnet.com/bpg/gerinfo/242>

STEPS FOR SUBMITTING MANUSCRIPTS

<https://www.wjgnet.com/bpg/GerInfo/239>

ONLINE SUBMISSION

<https://www.f6publishing.com>

Basic Study

BRAF^{V600E} mutant colorectal cancer cells mediate local immunosuppressive microenvironment through exosomal long noncoding RNAs

Jie Zhi, Xiao-Jing Jia, Jing Yan, Hui-Cong Wang, Bo Feng, Han-Ying Xing, Yi-Tao Jia

ORCID number: Jie Zhi 0000-0003-1727-7746; Xiao-jing Jia 0000-0003-1783-1292; Jing Yan 0000-0002-0082-2747; Hui-Cong Wang 0000-0003-2023-5176; Bo Feng 0000-0002-5758-9130; Han-Ying Xing 0000-0002-0337-9541; Yi-Tao Jia 0000-0003-2610-9330.

Author contributions: Jia YT made substantial contributions to the conception and design of the study; Zhi J searched and reviewed published articles and wrote the manuscript; Jia XJ and Yan J collected patient data and prepared the tables; Zhi J, Jia XJ, Yan J and Wang HC performed the relevant experiments in the manuscript, statistically analyzed the data, and prepared the figures; Feng B and Xing HY critically reviewed the article and made revisions to the manuscript; all authors approved the final version.

Institutional review board statement: The study was reviewed and approved by the Hebei General Hospital Institutional Review Board (approval No. 202134).

Conflict-of-interest statement: The authors report no conflicts of interest for this manuscript.

Jie Zhi, Hui-Cong Wang, Bo Feng, Yi-Tao Jia, Department of Oncology, Hebei General Hospital, Shijiazhuang 050051, Hebei Province, China

Xiao-Jing Jia, Department of Oncology, The First Hospital of Shijiazhuang, Shijiazhuang 050051, Hebei Province, China

Jing Yan, Department of Oncology, Puyang People's Hospital, Puyang 457000, Henan Province, China

Han-Ying Xing, Clinical Medical Research Center, Hebei General Hospital, Shijiazhuang 050051, Hebei Province, China

Corresponding author: Yi-Tao Jia, MD, Professor, Department of Oncology, Hebei General Hospital, No. 348 Heping West Road, Shijiazhuang 050051, Hebei Province, China. jiayitao99@163.com

Abstract**BACKGROUND**

BRAF^{V600E} mutated colorectal cancer (CRC) is prone to peritoneal and distant lymph node metastasis and this correlates with a poor prognosis. The BRAF^{V600E} mutation is closely related to the formation of an immunosuppressive microenvironment. However, the correlation between BRAF^{V600E} mutation and changes in local immune microenvironment of CRC is not clear.

AIM

To explore the effect and mechanism of BRAF^{V600E} mutant on the immune microenvironment of CRC.

METHODS

Thirty patients with CRC were included in this study: 20 in a control group and 10 in a treatment group. The density of microvessels and microlymphatic vessels, and M2 subtype macrophages in tumor tissues were detected by immunohistochemistry. Screening and functional analysis of exosomal long noncoding RNAs (lncRNAs) were performed by transcriptomics. The proliferation and migration of human umbilical vein endothelial cells (HUVECs) and human lymphatic endothelial cells (HLECs) were detected by CCK-8 assay and scratch test,

Data sharing statement: No additional data are available.

Country/Territory of origin: China

Specialty type: Oncology

Provenance and peer review:

Unsolicited article; Externally peer reviewed.

Peer-review report's scientific quality classification

Grade A (Excellent): 0

Grade B (Very good): 0

Grade C (Good): 0

Grade D (Fair): 0

Grade E (Poor): 0

Open-Access: This article is an open-access article that was selected by an in-house editor and fully peer-reviewed by external reviewers. It is distributed in accordance with the Creative Commons Attribution NonCommercial (CC BY-NC 4.0) license, which permits others to distribute, remix, adapt, build upon this work non-commercially, and license their derivative works on different terms, provided the original work is properly cited and the use is non-commercial. See: <http://creativecommons.org/licenses/by-nc/4.0/>

Received: July 13, 2021

Peer-review started: July 13, 2021

First decision: August 9, 2021

Revised: August 18, 2021

Accepted: October 25, 2021

Article in press: October 25, 2021

Published online: December 15, 2021

P-Reviewer: Saber A

S-Editor: Gao CC

L-Editor: Wang TQ

P-Editor: Gao CC



respectively. The tube-forming ability of endothelial cells was detected by tube formation assay. The macrophage subtypes were obtained by flow cytometry. The expression of vascular endothelial growth factor (VEGF)-A, basic fibroblast growth factor (bFGF), transforming growth factor (TGF)- β 1, VEGF-C, claudin-5, occludin, zonula occludens (ZO)-1, fibroblast activation protein, and α -smooth muscle actin was assessed by western blot analysis. The levels of cytokines interleukin (IL)-6, TGF- β 1, and VEGF were assessed by enzyme-linked immunosorbent assay.

RESULTS

BRAF^{V600E} mutation was positively correlated with the increase of preoperative serum carbohydrate antigen 19-9 ($P < 0.05$), and with poor tumor tissue differentiation in CRC ($P < 0.01$). Microvascular density and microlymphatic vessel density in BRAF^{V600E} mutant CRC tissues were higher than those in BRAF wild-type CRC ($P < 0.05$). The number of CD163⁺M2 macrophages in BRAF^{V600E} mutant CRC tumor tissue was markedly increased ($P < 0.05$). Compared with exosomes from CRC cells with BRAF gene silencing, the expression of 13 lncRNAs and 192 mRNAs in the exosomes from BRAF^{V600E} mutant CRC cells was upregulated, and the expression of 22 lncRNAs and 236 mRNAs was downregulated ($P < 0.05$). The biological functions and signaling pathways predicted by differential lncRNA target genes and differential mRNAs were closely related to angiogenesis, tumor cell proliferation, differentiation, metabolism, and changes in the microenvironment. The proliferation, migration, and tube formation ability of HUVECs and HLECs induced by exosomes in the 1627 cell group (HT29 cells with BRAF gene silencing) was greatly reduced compared with the HT29 cell group ($P < 0.05$). Compared with the HT29 cell group, the expression levels of VEGF-A, bFGF, TGF- β 1, and VEGF-C in the exosomes derived from 1627 cells were reduced. The expression of ZO-1 in HUVECs, and claudin-5, occludin, and ZO-1 in HLECs of the 1627 cell group was higher. Compared with the 1627 cell group, the exosomes of the HT29 cell group promoted the expression of CD163 in macrophages ($P < 0.05$). IL-6 secretion by macrophages in the HT29 cell group was markedly elevated ($P < 0.05$), whereas TGF- β 1 was decreased ($P < 0.05$). The levels of IL-6, TGF- β 1, and VEGF secreted by fibroblasts in the 1627 cell group decreased, compared with the HT29 cell group ($P < 0.05$).

CONCLUSION

BRAF^{V600E} mutant CRC cells can reach the tumor microenvironment by releasing exosomal lncRNAs, and induce the formation of an immunosuppressive microenvironment.

Key Words: Colorectal cancer; BRAF^{V600E} mutant; Exosome; Long noncoding RNA; Immunosuppressive microenvironment

©The Author(s) 2021. Published by Baishideng Publishing Group Inc. All rights reserved.

Core Tip: This study revealed that BRAF^{V600E} mutant colorectal cancer (CRC) cells could lead to more angiogenesis and lymphoangiogenesis in the microenvironment by releasing exosomal long noncoding RNAs, inducing the formation of an immunosuppressive microenvironment. Our findings provide a hypothesis for finding new therapeutic strategies for BRAF^{V600E} mutant CRC.

Citation: Zhi J, Jia XJ, Yan J, Wang HC, Feng B, Xing HY, Jia YT. BRAF^{V600E} mutant colorectal cancer cells mediate local immunosuppressive microenvironment through exosomal long noncoding RNAs. *World J Gastrointest Oncol* 2021; 13(12): 2129-2148

URL: <https://www.wjgnet.com/1948-5204/full/v13/i12/2129.htm>

DOI: <https://dx.doi.org/10.4251/wjgo.v13.i12.2129>

INTRODUCTION

Colorectal cancer (CRC) is one of the most common malignant tumors, and ranks third in morbidity and mortality globally[1]. In China, societal and lifestyle changes have tended to increase the morbidity and mortality of CRC[2]. BRAF^{V600E} gene mutation accounts for approximately 10% of patients with metastatic CRC (mCRC), and is a point mutation at nucleotide 1799 of exon 15 (T mutated into A), resulting in a change of the encoded amino acid 600, valine replaced by glutamate (V600E)[3,4]. BRAF^{V600E} mutation can continuously activate the RAS-RAF-MEK-ERK signaling pathway, promote tumor cell proliferation and migration, and induce angiogenesis, thereby reducing tumor cell apoptosis[5-8]. Clinical data reveal that BRAF^{V600E} mutation frequently occurs in elderly women, and the related pathological type is mostly mucinous adenocarcinoma with a high level of tissue differentiation. Around 20% of patients have accompanying microsatellite instability, and most of them develop right colon cancer originating from serrated adenomas[4,9]. Compared with wild-type BRAF, patients with BRAF^{V600E} mutant CRC are prone to peritoneal metastasis and distant lymph node metastasis with a poor prognosis. Generally, the median survival time is < 12 mo. The effective treatment rate reaches only approximately 20%, even with three-drug chemotherapy and targeted combination therapy[10,11]. It is therefore important to explore the mechanism of BRAF^{V600E} mutant CRC with lymph node and peritoneal metastasis and to discover effective therapeutic strategies. This may be applicable to start with its specific immune microenvironment.

The tumor microenvironment (TME) is the local environment facilitating tumor growth and proliferation[12]. In thyroid cancer, the proportion of mast cells in BRAF^{V600E} mutant TME is markedly increased compared with wild-type BRAF, which may be involved in mediating the formation of the immunosuppressive microenvironment, suggesting that BRAF^{V600E} mutation affects the TME[13]. Multiple cells (namely, endothelial cells, fibroblasts, and immune cells) and extracellular components (namely, cytokines, growth factors, hormones, and extracellular matrix) in the TME can induce tumor angiogenesis and lymphangiogenesis and promote chronic inflammation, thereby creating a local immunosuppressive microenvironment, which plays a vital role in tumor occurrence, invasion, and metastasis and drug resistance[14]. Tumor-associated macrophages (TAMs) and cancer-associated fibroblasts (CAFs) are the principal components of the TME. Among them, M2-type macrophages have an immunosuppressive effect. They can promote tumor cell proliferation, infiltration, and metastasis, and their expression level is intimately associated with patient prognosis [15,16]. Meanwhile, CAFs have undergone substantial changes in morphology, proliferation activity, motility, and secretory function, which can facilitate tumor proliferation, invasion, metastasis, and angiogenesis, and their expression level is closely linked to tumor stage and poor prognosis[17]. There is no current research investigating the relationship between BRAF^{V600E} gene mutation and the formation and functional changes of blood vessels, lymphatic vessels, TAMs, and CAFs in the CRC local immune microenvironment.

Exosomes are a type of cystic microvesicle secreted by cells, and the secretion process is active. They are able to carry specific biologically active molecules including lipids, miRNA, and long noncoding RNAs (lncRNAs) into the corresponding target cells and mediate substance transportation and information exchange intercellularly [18]. lncRNAs belong to a class of single-stranded RNA molecules that do not encode proteins. They play a role *via* transcription, post-transcription, and translation, and participate in tumor occurrence, invasion, and metastasis. Exosomes secreted by tumor cells can modify the TME through lncRNAs, thereby promoting the development of tumors[19,20]. Liang *et al*[21] noted that the expression of exosome-derived lncRNA RPPH1 in CRC was markedly upregulated. It can prevent ubiquitination by binding to TUBB3 and induce epithelial-mesenchymal transition, and interact with TAMs to promote the polarization of TAMs to M2 subtype, thereby accelerating tumor progression. However, there is still a lack of relevant investigations on whether BRAF^{V600E} mutant CRC cells affect the TME through the release of exosomal lncRNAs.

The present study aimed to investigate the influence of BRAF^{V600E} mutation in CRC on the surrounding immune microenvironment, and to elucidate whether BRAF^{V600E} mutant CRC cell-derived exosomes participate in the formation of an immunosuppressive microenvironment. It is hoped that the results will provide a novel therapeutic strategy for BRAF^{V600E} mutant CRC.

MATERIALS AND METHODS

General information

Data of ten BRAF^{V600E} mutant CRC patients who underwent surgical treatment at the Hebei General Hospital from September 2014 to June 2019 were collected. Twenty BRAF wild-type CRC patients were selected as controls. There were 18 male and 12 female patients. The age range was 27-79 years, with an average of 57.57 ± 2.13 years and median of 57 years. The specimens were obtained with informed consent obtained from the patients and under the approval of the Ethics Committee of the Fourth Hospital of Hebei Medical University. The inclusion criteria were: (1) Patients with a pathological diagnosis of CRC, in whom those identified as having BRAF^{V600E} mutation were included in an experimental group, and those identified as having wild-type BRAF were included in a control group; (2) Untreated patients; and (3) Undergoing first surgical treatment for primary CRC. The exclusion criteria were: (1) History of malignant tumors; (2) Current primary tumors in other regions; and (3) Patients with incomplete pathological data.

Cells and reagents

The human colon cancer cell line HT29 (BRAF^{V600E} mutant) was purchased from the Cell Bank of the Chinese Academy of Sciences. The human colon cancer cell line 1627 was obtained from Shanghai GenePharma Company, which was a HT29 cell strain with the BRAF gene being silenced. Human umbilical vein endothelial cells (HUVECs) and human lymphatic endothelial cells (HLECs) were purchased from ScienCell, San Diego, CA, United States. Human monocytic leukemia cells (THP-1 cells) and human embryonic lung fibroblasts (MRC-5 cells) were obtained from the Cell Bank of the Shanghai Institutes for Biological Sciences, Chinese Academy of Sciences. McCoy's 5A, RPMI 1640, minimal essential medium, and fetal bovine serum (FBS) were all purchased from Gibco (NY, United States).

Induction of macrophages

THP-1 cells in the logarithmic phase of growth were obtained and placed in a 15-mL centrifuge tube, and centrifuged at 1000 r/min for 5 min. The supernatant was discarded. Following addition of fresh RPMI 1640 culture medium, the cells were resuspended and inoculated in a 12-well plate with 5×10^5 cells per well, supplemented with pharmaceutical manufacturers association (PMA) solution (dissolved in DMSO) (Cayman, MI, United States) at a final concentration of 100 ng/mL, and cultured in a constant temperature incubator for 48 h. The cells were ultimately placed under a biological microscope (Nikon, Tokyo, Japan) and the cell morphology and adhesion were observed.

Immunohistochemistry

The postoperative tissue samples of CRC patients were collected, embedded in paraffin, and cut into 5-mm sections. After deparaffinization and hydration, antigen retrieval, and incubation in 3% H₂O₂ for 10 min, the corresponding antibodies were added, including rabbit anti-human CD31 monoclonal antibody (1:2000, Arigo, Hsinchu City, Taiwan), rabbit LYVE-1 polyclonal antibody (1:200, Arigo), mouse anti-human CD68 monoclonal antibody (1:100, BD Biosciences, NJ, United States), rabbit anti-human CD163 monoclonal antibody (1:100, HUABIO, Hangzhou, China), and rabbit anti-human α -smooth muscle actin (SMA) monoclonal antibody (1:100, HUABIO). 3,3-diaminobenzidine (DAB) color development was performed for microscopic observation. A double-blind reading method was adopted by two pathologists. The sections were initially visualized under low magnification ($\times 100$) to determine three fields where cells were most densely distributed. The number of positive cells was counted under high magnification ($\times 400$), and the average number was calculated.

Extraction and identification of exosomes

Cell supernatant was collected and centrifuged at $480 \times g$ for 5 min, followed by $2000 \times g$ for 10 min to remove cell debris. The supernatant was collected and centrifuged at $10000 \times g$ for 30 min to remove macrovesicles. The supernatant was collected again and centrifuged at $100000 \times g$ for 2 h. The supernatant was discarded and the exosomes were resuspended in 200 mL of PBS solution, and stored in a freezer at -80°C for later use. The morphology of exosomes was identified with a transmission electron microscope (Hitachi, Tokyo, Japan). At room temperature, 10 mL of exosome suspension was dripped on a 2-nm-pore-diameter copper mesh using a pipette and

allowed to stand for 2 min. The liquid was absorbed dry using absorbent paper. A quantity of 30 mL 3% tungsten phosphate was dripped onto the copper mesh for negative staining for 5 min, and the liquid was absorbed dry using absorbent paper. After drying, photographs were taken under a transmission electron microscope.

Western blot analysis

The cell samples were removed from the -80 °C freezer and supplemented with 200 mL of RIPA lysis solution for 20 min to extract the total cell proteins. The BCA protein concentration determination kit was used to quantify the proteins. The proteins were subjected to SDS-PAGE, transferred to polyvinylidene difluoride (PVDF) membranes at 250 mA, and blocked with bovine serum albumin for 2 h. The blocked PVDF membranes were placed directly into the freshly prepared primary antibody working solution at 4 °C overnight. Primary antibodies used included rabbit anti-human CD9 monoclonal antibody (1:1000, Abcam, Cambridge, United Kingdom), rabbit anti-human CD63 monoclonal antibody (1:5000, Abcam), rabbit anti-human BRAF monoclonal antibody (1:1000, Arigo), rabbit anti-zonula occludens (ZO)-1 polyclonal antibody (1:1000, GenTex, Gentex, United States), rabbit anti-claudin-5 polyclonal antibody (1:1000, GenTex), rabbit anti-occludin polyclonal antibody (1:1000, HUABIO), rabbit anti-transforming growth factor (TGF)-1 polyclonal antibody (1:1000, Bioss, Beijing, China), rabbit anti-vascular endothelial growth factor (VEGF)-C polyclonal antibody (1:800, Bioworld, MN, United States), rabbit anti-basic fibroblast growth factor (anti-bFGF) polyclonal antibody (1:600, Bioss), mouse anti-human VEGF-A monoclonal antibody at a concentration of 6 mg/mL (Abcam), rabbit anti-human fibroblast activation protein (FAP) monoclonal antibody (1:1000, Abcam), and rabbit anti-human α -SMA monoclonal antibody (1:1000, Abcam). Following membrane washing on the next day, the corresponding secondary antibody was incubated, and chemiluminescence was detected with ECL substrate. After developing and fixing, the film was scanned using a scanner, and Tanon 1600 software was used for gray scale analysis and quantification.

CCK-8 assay

Cells in the logarithmic phase of growth were selected and seeded in a 96-well plate at 5×10^3 cells/well with a volume of 100 μ L per well, and cultured at 37 °C in a 5% CO₂ incubator. After 6 h of inoculation, the experimental group was treated with 10 mL exosomes, and the control group with 10 mL PBS solution, and then cultured in the incubator again. Exosomes were cocultured with HUVECs for 24, 48, and 72 h, and cocultured with HLECs for 12, 24 and 36 h; 10 mL of CCK-8 reagent (DOJINDO, Kyushu, Japan) was added to each well and incubated at 37 °C with 5% CO₂ for 1 h. Absorbance at 560 nm was measured using a microplate reader (ThermoFisher Scientific, MA, United States).

Scratch test

HUVECs or HLECs were plated in six-well plates. When the cells were evenly spread, they were scratched using a 200- μ L pipette tip. PBS solution was used to rinse once for the removal of the suspended cells. To each well, 2 mL of FBS-free culture medium was added. The experimental group was supplemented with 20 μ L of exosomes, and the control group with 20 μ L of PBS solution. Both groups were cultured at 37 °C in a 5% CO₂ incubator. The cells were observed and photographed under a microscope at 0 and 24 h, respectively, to detect the scratch healing. Cell migration rate was calculated as [(scratch area at 0 h - scratch area at 24 h)/scratch area at 0 h] \times 100%.

Tube formation assay

After freezing and thawing the Matrigel matrix (BD Biosciences, United States) containing low levels of growth factors at 4 °C, the homogenate was mixed well with a precooled pipette tip and packaged into precooled Eppendorf tubes. Matrigel matrix was diluted with serum-free medium at a ratio of 1:3, and the 96-well plate was placed on an ice pack. Fifty microliters of diluted Matrigel matrix was added to each well and left to stand at 37 °C for 30 min. Cells were seeded in a 96-well plate at 10^4 cells/well and supplemented with 100 μ L cell suspension in each well. The experimental group was treated with 10 μ L of exosomes, and the control group with 10 μ L PBS solution, and then cultured at 37 °C in a 5% CO₂ incubator. After culturing for 24 h, the cells were visualized and photographed under a low magnification (\times 100) microscope and the tube formation ability of endothelial cells was observed.

Flow cytometry

THP-1 cells were induced with PMA for 48 h and the culture medium was discarded following three cycles of washing with PBS. Trypsin (0.5 mL) was supplied to each well for digestion, and 1.5 mL of culture medium containing 10% FBS was utilized to terminate the digestion. The cells were then collected and centrifuged at 1000 r/min for 5 min. The supernatant was discarded, and the cells were resuspended in PBS and centrifuged again to obtain the precipitate. Mouse anti-human CD68 monoclonal antibody (5 μ L; BD Biosciences) and rabbit anti-human CD163 monoclonal antibody (5 μ L; BD Biosciences) were added and incubated at 4 °C in the dark for 30 min. Following two cycles of washing with PBS, the cells were centrifuged at 1000 r/min for 5 min, resuspended in 300 μ L PBS, and loaded on a flow cytometer (Beckman Coulter, CA, United States) for determination.

Enzyme-linked immunosorbent assay

After cells were cultured for 48 h, the medium was collected and centrifuged at 1000 r/min for 5 min. An enzyme-linked immunosorbent assay (ELISA) kit (MULTI SCIENCES, Hangzhou, China) was used to detect the expression of interleukin (IL)-6, TGF- β 1, and VEGF in the culture medium. IL-6 antibody, TGF- β 1 antibody, VEGF antibody, and horseradish peroxidase-labeled streptavidin were all diluted 1:100.

Extraction and identification of exosomal RNA

AllPrep RNA/LncRNA kit (Qiagen, Hilden, Germany) was used to extract total RNA from exosomes. The purity of RNA was determined using QubitRNA kit (Thermo Fischer Scientific). The RNA concentration was accurately quantified utilizing Qubit. The integrity of RNA was assessed using Agilent 2100.

Transcriptome library preparation, sequencing, and data analysis

Exosome samples of HT29 and 1627 cells were initially obtained and total exosomal RNA was extracted. Ovation Solo RNA kit (NugEN) was used for library construction of exosomal lncRNAs. The constructed library was sequenced through the Illumina HiSeq 4000 platform where the double-terminal 250-300 nt transcripts were generated. The raw data in Fastq format were processed using perl to obtain sequencing data. By logging in to the TopHat2 system, the sequenced data transcripts were aligned and analyzed in light of the reference genome. Cufflinks software was used to compare the analyzed data for transcript splicing and the transcriptome was obtained. Quantitative analysis was performed on the transcript. Finally, the transcript data set was retrieved using the RefSeq database as an mRNA data set. Cuffmerge software was used to merge the obtained transcripts after splicing, delete the transcripts with unclear mid-strand direction, and obtain a mRNA transcript data set. lncRNAs were ultimately screened from the combined transcript set.

Prediction of lncRNA target genes and GO and KEGG enrichment analysis

The target genes of lncRNAs were predicted through cis-acting and trans-acting, including annotating the function of its target gene mRNA. The GO seq software and KOBAS software were used to enrich differential lncRNA target genes and differential mRNAs in the three processes of biological process, cell component, and molecular function. The biological functions involved in differential lncRNA target genes and differential mRNAs were analyzed. KOBAS software was used to enrich the differential lncRNA target genes and differential mRNAs with KEGG pathways. The signal transduction pathways involved in differential lncRNA target genes and differential mRNA were also analyzed.

Statistical analysis

SPSS 21.0 software was used for statistical analyses. Enumerative data are expressed as percentages and analyzed using the χ^2 test or Fisher's exact test. The enumerative data are expressed as the mean \pm SD. The two groups of enumerative data were tested by two independent samples *t*-tests. One-way analysis of variance was applied for multiple groups of samples. *P* < 0.05 was considered statistically significant.

RESULTS

Relationship between BRAF^{V600E} mutation and clinicopathological parameters

We collected and analyzed the clinical data of 10 BRAF^{V600E} mutant and 20 BRAF wild-type CRC patients. In CRC, BRAF^{V600E} mutation was positively correlated with the increase of preoperative serum carbohydrate antigen (CA)19-9 ($P < 0.05$), and it was correlated with poor tumor tissue differentiation ($P < 0.01$). However, no correlation was revealed with gender, age, location, mucous tissue, T stage, TNM stage, lymph node metastasis, nerve invasion, vascular tumor thrombus, preoperative carcinoembryonic antigen (CEA) level, or preoperative platelet count of the patients (Table 1).

BRAF^{V600E} mutation promotes formation of microvessels and microlymphatic vessels in tumor tissues and increases infiltration of M2 macrophages

To explore the influence of BRAF^{V600E} mutation on the TME, we identified the formation of tumor blood vessels and lymph vessels in BRAF^{V600E} mutation and BRAF wild-type CRC tissues. Microvascular density (MVD) and microlymphatic vessel density (MLVD) in BRAF^{V600E} mutant CRC tissues were higher than those in BRAF wild-type CRC ($P < 0.05$) (Figure 1A and Table 2). The number of CD163⁺M2 macrophages in BRAF^{V600E} mutant CRC tumor tissue was markedly increased ($P < 0.05$) (Figure 1B and Table 3), whereas the number of CD68⁺M1 macrophages was not significantly different (Figure 1B and Table 3). Additionally, the density of fibroblasts exhibited no significant difference (Figure 1C and Table 4). These results suggest that BRAF^{V600E} mutation promotes the formation of microvessels and microlymphatic vessels in tumor tissues, increases the infiltration of M2 macrophages, and induces an immunosuppressive microenvironment.

BRAF^{V600E} mutant CRC cells can reach the TME by releasing exosomal lncRNAs, and induce formation of an immunosuppressive microenvironment

We performed transcriptomics analysis on exosomes derived from BRAF^{V600E} mutant CRC cells and those with BRAF gene silencing. Compared with the exosomes from cells with BRAF gene silencing, the expression of 13 lncRNAs and 192 mRNAs in the exosomes of BRAF^{V600E} mutant CRC cells was upregulated, and the expression of 22 lncRNAs and 236 mRNAs was downregulated ($P < 0.05$) (Figure 2A). Using cluster analysis charts, the distribution of differentially expressed lncRNAs and mRNAs in exosomes of BRAF^{V600E} mutant CRC cells and those with BRAF gene silencing was further exhibited (Figure 2B).

To illustrate the biological functions of differential lncRNAs and mRNAs and the signaling pathways involved, we conducted GO enrichment analysis and KEGG signaling pathway analysis. GO enrichment analysis included three aspects of biological process, cell component, and molecular function. Differential lncRNA target genes and mRNAs presented similar biological functions, and they are mainly involved in nucleic acid metabolism, macromolecular metabolism, nitride metabolism, and RNA metabolism. Cellular components include mostly the formation of nuclei, organelles, and nucleosomes. Molecular functions involve regulation of cell adhesion, cytoskeletal remodeling, gene expression regulation, and protein binding (Figure 2C).

KEGG results indicated that the target genes of differential lncRNAs were mainly involved in the p53 pathway, ErbB pathway, steroid synthesis pathway, actin cytoskeleton regulation pathway, pyruvate metabolism pathway, cell cycle regulation pathway, and the pathway of protein processing in the endoplasmic reticulum (Figure 2D). Differential mRNAs are mainly involved in the VEGF pathway, mammalian target of rapamycin pathway, mitogen-activated protein kinase pathway, and the pathway of protein processing in the endoplasmic reticulum (Figure 2D). The biological functions and signaling pathways predicted by differential lncRNA target genes and differential mRNAs coincided with each other. Furthermore, it was closely related to angiogenesis, tumor cell proliferation, differentiation, metabolism, and changes in the microenvironment, suggesting that BRAF^{V600E} mutant CRC cells could reach the TME by releasing exosomal lncRNAs, and induce formation of an immunosuppressive microenvironment through mRNAs.

BRAF^{V600E} mutant CRC cell-derived exosomes promote proliferation, migration, and tube formation of HUVECs and HLECs, and induce angiogenesis and lymphoangiogenesis

Exosomes derived from HT29 and 1627 cells were cocultured with HUVECs or HLECs to detect cell proliferation. OD values of HUVECs in the HT29 group and 1627 group

Table 1 Relationship between BRAF^{V600E} mutation and clinicopathological parameters in colorectal cancer

Variable	Cases (%)	BRAF ^{V600E} mutation		P value
		Yes (%)	No (%)	
Gender				
Male	18 (60)	6 (60)	12 (60)	0.326
Female	12 (40)	4 (40)	8 (40)	
Age (yr)				
≥ 65	10 (33.3)	4 (40)	6 (30)	0.440
< 65	20 (66.7)	6 (60)	14 (70)	
Location				
Right colon	9 (30)	2 (20)	7 (35)	0.345
Left colon	9 (30)	5 (50)	4 (20)	
Rectum	12 (40)	3 (30)	9 (45)	
Mucous tissue				
Positive	6 (20)	1 (10)	5 (25)	0.326
Negative	24 (80)	9 (90)	15 (75)	
Differentiated degree				
High/moderate differentiation	20 (66.7)	3 (30)	17 (85)	0.005 ^a
Poor differentiation	10 (33.3)	7 (70)	3 (15)	
T stage				
T2	4 (13.3)	0	4 (20)	0.211
T3	3 (10)	2 (20)	1 (5)	
T4	23 (76.7)	8 (80)	15 (75)	
TNM stage				
I + II	13 (43.3)	2 (20)	11 (55)	0.074
III + IV	17 (56.7)	8 (80)	9 (45)	
Lymph node				
Positive	17 (56.7)	8 (80)	9 (45)	0.074
Negative	13 (43.3)	2 (20)	11 (55)	
Nerve invasion				
Positive	7 (23.3)	4 (40)	3 (15)	0.143
Negative	23 (76.7)	6 (60)	17 (85)	
Vessel carcinoma embolus				
Positive	3 (10)	1 (10)	2 (10)	0.652
Negative	27 (90)	9 (90)	18 (90)	
CA19-9 (U/mL)				
High	12 (40)	7 (70)	5 (25)	0.024 ^a
Normal	18 (60)	3 (30)	15 (75)	
CEA (ng/mL)				
High	11 (36.7)	3 (30)	8 (40)	0.452
Normal	19 (63.3)	7 (70)	12 (60)	
PLT count (× 10 ⁹ /L)				
High	12 (40)	5 (50)	7 (35)	0.344

Normal	18 (60)	5 (50)	13 (65)
--------	---------	--------	---------

^a*P* < 0.05.

PLT: Platelets; CEA: Carcinoembryonic antigen; CA19-9: Carbohydrate antigen 19-9.

Table 2 Relationship between BRAF^{V600E} mutation and microvascular density/microlymphatic vessel density in colorectal cancer

BRAF ^{V600E} mutation	MVD		MLVD	
	mean ± SD	<i>P</i> value	mean ± SD	<i>P</i> value
+	38.53 ± 17.11	0.030	9.67 ± 5.63	0.0001
-	27.54 ± 9.54		3.81 ± 2.06	

MVD: Microvascular density; MLVD: Microlymphatic vessel density.

Table 3 Relationship between BRAF^{V600E} mutation and tumor-associated macrophages in colorectal cancer

BRAF ^{V600E} mutation	CD68 ⁺ macrophage		CD163 ⁺ M2 macrophage	
	mean ± SD	<i>P</i> value	mean ± SD	<i>P</i> value
+	18.43 ± 13.53	0.664	8.33 ± 5.93	0.040
-	20.96 ± 15.34		3.67 ± 3.02	

Table 4 Relationship between BRAF^{V600E} mutation and cancer-associated fibroblasts in colorectal cancer

BRAF ^{V600E} mutation	CAFs		<i>P</i> value
	Low expression (cases)	High expression (cases)	
+	2	8	1
-	3	17	

CAF: Cancer-associated fibroblast.

at 24 h were 1.215 ± 0.032 and 0.986 ± 0.046 , respectively; 1.563 ± 0.035 and 1.200 ± 0.163 at 48 h, respectively; and 1.661 ± 0.031 and 1.369 ± 0.020 at 72 h, respectively. At 24, 48 and 72 h, HUVEC proliferation induced by exosomes in the 1627 cell group was reduced compared with the HT29 cell group (*P* < 0.05), but there was no significant difference in HUVEC proliferation between the 1627 cell group and control group (Figure 2A). The OD values of HLECs in the control group, HT29 cell group, and 1627 cell group at 12 h were 0.477 ± 0.006 , 0.526 ± 0.007 , and 0.500 ± 0.004 , respectively; 0.622 ± 0.003 , 0.728 ± 0.010 , and 0.680 ± 0.010 at 24 h, respectively; and 0.644 ± 0.006 , 0.725 ± 0.009 , and 0.682 ± 0.014 at 36 h, respectively. At 12, 24, and 36 h, the proliferation of HLECs induced by exosomes in the 1627 cell group was greatly reduced compared with the HT29 cell group (*P* < 0.05) and the proliferation of HLECs in the 1627 cell group was greater than that of the control group (*P* < 0.05) (Figure 3A).

Light microscopy indicated that the average migration rate of HUVECs in the HT29 cell group was $82.863\% \pm 3.095\%$ and that of the 1627 cell group was $45.067\% \pm 2.895\%$ at 24 h after scratch. The average migration rate of HLECs in the HT29 cell group was $42.393\% \pm 0.247\%$, and that of the 1627 cell group was $23.327\% \pm 1.434\%$. Compared with the 1627 cell group, the migration of HUVECs and HLECs induced by exosomes in the HT29 cell group was substantially elevated (*P* < 0.01) (Figure 3B).

After 24 h of incubation, the average number of tube formations by HUVECs in the HT29 cell group and 1627 cell group was 30.625 ± 0.925 and 12.750 ± 1.887 , respectively, at low magnification. The average number of tube formations by HLECs in the HT29 cell group and 1627 cell group was 26.750 ± 2.016 and 15.375 ± 1.413 , respectively, at low magnification. Compared with the 1627 cell group, the tube formation ability of HUVECs and HLECs induced by exosomes in the HT29 cell group

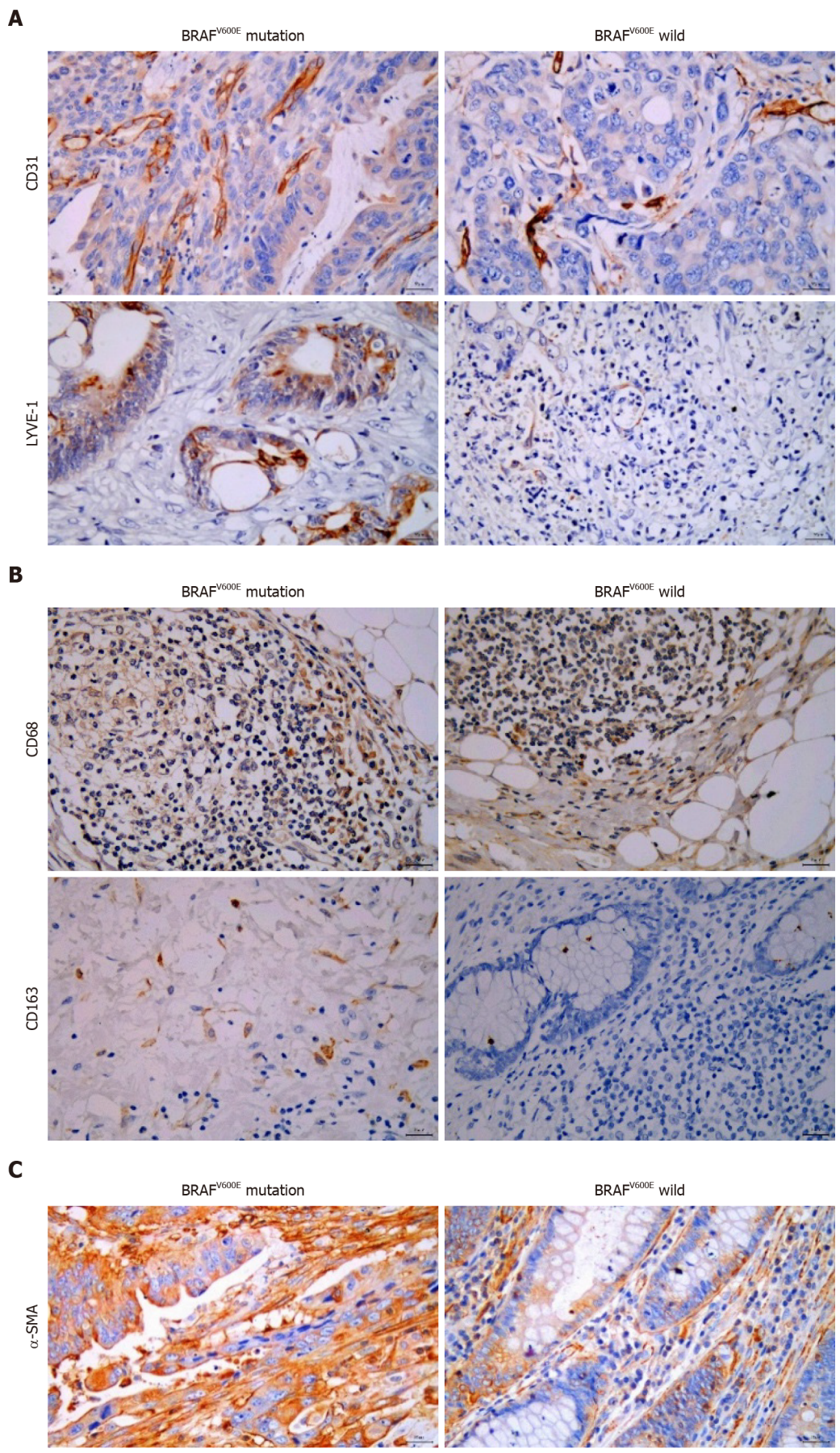


Figure 1 Relationship between BRAF^{V600E} mutation and microvascular density, microlymphatic vessel density, tumor-associated macrophages, and cancer-associated fibroblasts. A: Expression of CD31 and lymphatic vessel endothelial hyaluronin acid receptor-1 (LYVE-1) in

BRAF^{V600E} mutant and BRAF wild type colorectal cancer (CRC) tissues (CD31 labeled microvascular density, and LYVE-1 labeled microlymphatic vessel density; immunohistochemistry, × 400); B: Expression of CD68 and CD163 proteins in BRAF^{V600E} mutant and BRAF wild type CRC tissues (CD68 labeled TAMs, and CD163 labeled M2 subtype macrophages; immunohistochemistry, × 400); C: Expression of α -SMA protein in BRAF^{V600E} mutant and BRAF wild type CRC tissues (α -SMA labeled CAFs; immunohistochemistry, × 400).

was markedly higher than that in the 1627 cell group ($P < 0.01$) (Figure 3C).

Western blot analysis indicated that compared with the HT29 cell group, the expression of VEGF-A, bFGF, TGF- β 1, and VEGF-C proteins in the exosomes derived from 1627 cells was reduced (Figure 3D). However, the expression of ZO-1 in HUVECs and that of claudin-5, occludin, and ZO-1 in HLECs in the 1627 cell group were higher than those in the HT29 cell group (Figure 3E and F). Neither the 1627 nor the HT29 group failed to display occludin and claudin-5 protein. This suggests that exosomes derived from BRAF^{V600E} mutant CRC cells promote angiogenesis and lymphoangiogenesis.

Exosomes derived from BRAF^{V600E} mutant CRC cells promote polarization of macrophages to M2 subtype and enhance secretory function of macrophages and fibroblasts

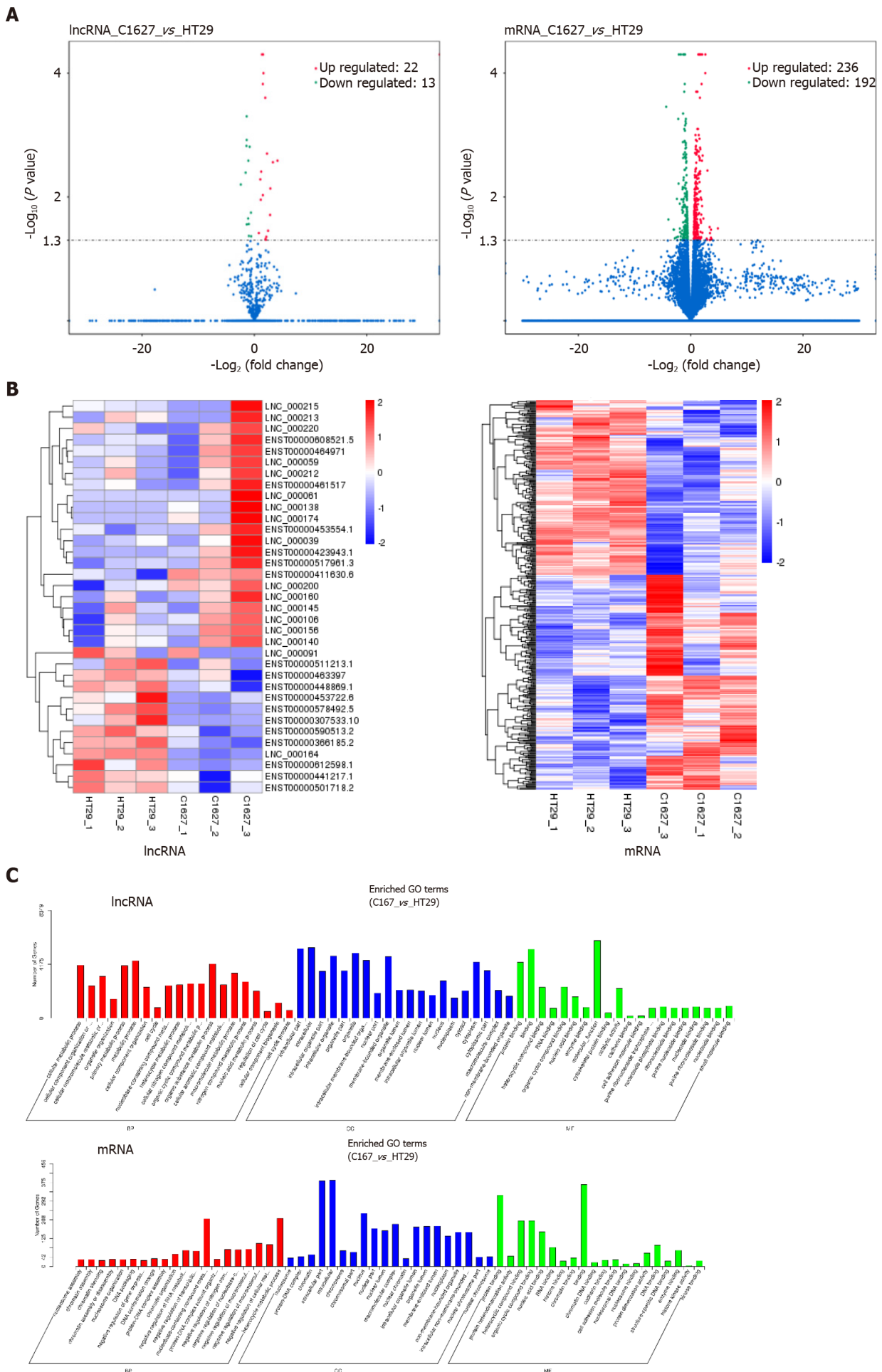
The exosomes derived from HT29 and 1627 cells were cocultured with macrophages. Flow cytometry revealed that the exosomes of the HT29 cell group promoted the expression of CD163 in macrophages compared with the control group and 1627 cell group ($P < 0.05$) (Figure 4A). ELISA indicated that IL-6 secreted by macrophages in the HT29 cell group was markedly elevated ($P < 0.05$), whereas TGF- β 1 was decreased ($P < 0.05$) (Figure 4B). Western blot analysis demonstrated that there was no significant difference in the expression of fibroblast FAP and α -SMA in the control, HT29 cell, and 1627 cell groups (Figure 4C). Conversely, the levels of IL-6, TGF- β 1, and VEGF secreted by fibroblasts in the 1627 cell group decreased, compared with the HT29 cell group ($P < 0.05$) (Figure 4D). Exosomes derived from BRAF^{V600E} mutant CRC cells promoted polarization of macrophages to M2 subtype and enhanced the secretory function of fibroblasts.

DISCUSSION

This study demonstrated that BRAF^{V600E} mutant CRC generates a unique immune microenvironment. Compared with BRAF wild type CRC, there was more angiogenesis and lymphoangiogenesis in the microenvironment. Meanwhile, the polarization of macrophages to M2 subtype was more obvious, and the immunosuppression was more prominent. Exosomes derived from BRAF^{V600E} mutant CRC cells could induce this change. Further analysis indicated that exosomes derived from BRAF^{V600E} mutant CRC cells were rich in certain lncRNAs and mRNAs, which might link to these alterations. Our findings suggested that for this particular CRC, it might be worthwhile to try to investigate the TME.

It is currently argued that BRAF^{V600E} mutation is of vital significance in predicting the prognosis of CRC patients[22]. Several studies have indicated that BRAF^{V600E} mutation is not only correlated to poor tissue differentiation, but also to gender, advanced stage, high T stage, right colon, lymph node metastasis, mucous tissue, and high levels of platelets and CEA[22,23]. Conversely, our results were inconsistent with those reported in the literature. We recognized that BRAF^{V600E} mutation was only associated with poor tissue differentiation and increased preoperative CA19-9 levels, which might have been caused by the small sample size.

However, we analyzed the TME of such patients. The results demonstrated that the MVD and MLVD in BRAF^{V600E} mutant CRC tissues were higher than those in BRAF wild type tissues, and the number of CD163⁺ M2 macrophages increased substantially. In papillary thyroid carcinoma, BRAF^{V600E} mutation upregulates the expression of VEGF-A in cancer cells and promotes angiogenesis, and increases the expression of VEGF-C in cancer cells and promotes lymphangiogenesis, whereas silencing BRAF gene can reverse these effects[24]. Under normal circumstances, HCT116 colon cancer cells can activate the VEGF signaling pathway, promote the proliferation, migration, and angiogenesis of vascular endothelial cells, and facilitate tumor metastasis by releasing exosomes[25]. Exosomes derived from CRC cells can also promote TAMs to release VEGF-C, enhance proliferation of lymphatic endothelial cells, and induce



D

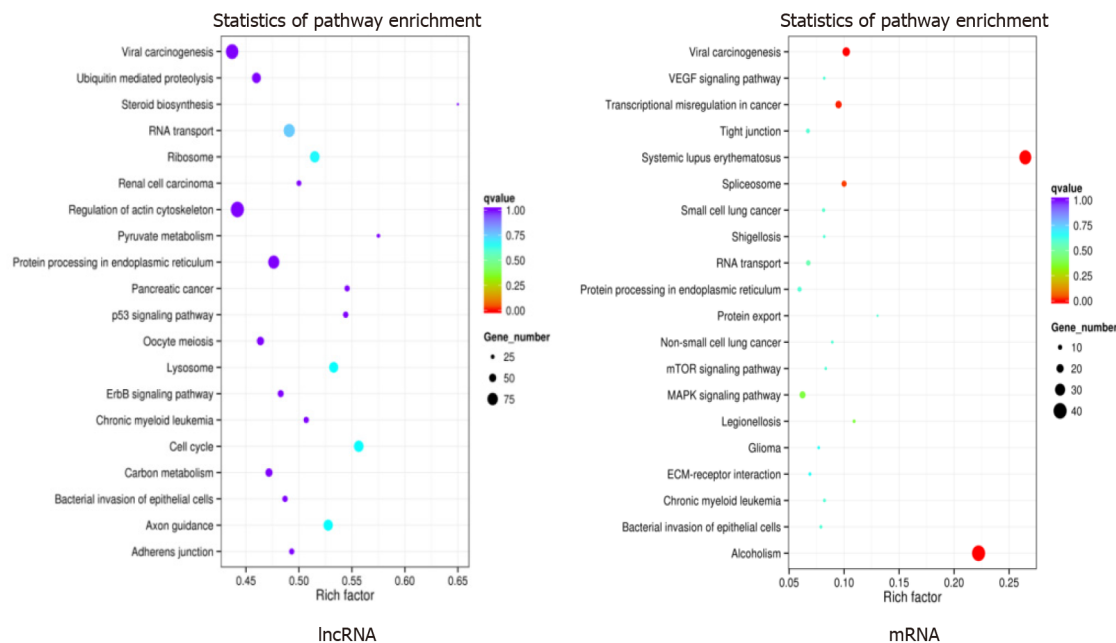


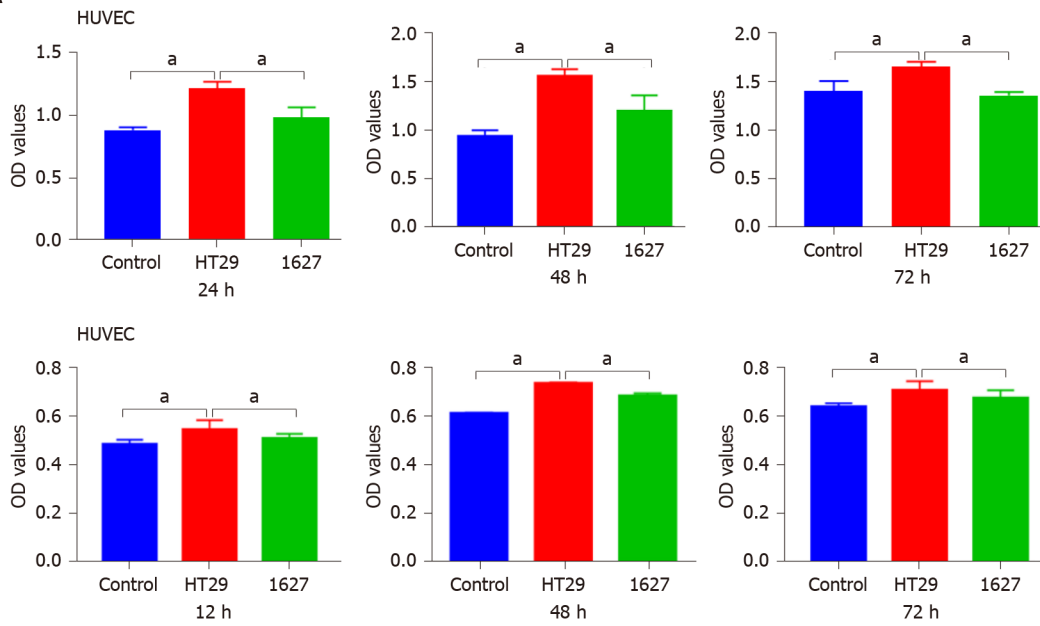
Figure 2 Screening and functional analysis of differentially expressed long noncoding RNAs and mRNAs in exosomes of BRAF^{V600E} mutant colorectal cancer cells and those with BRAF gene silencing. A: Transcriptomics analysis of differentially expressed long noncoding RNAs (lncRNAs) and mRNAs in the exosomes of HT29 and 1627 cells. Volcano maps are shown (the x axis represents the multiple of difference, and the y axis P values); B: Hierarchical cluster analysis of differentially expressed lncRNAs and mRNAs (red represents upregulated expression, and blue represents downregulated expression); C: GO enrichment analysis of differentially expressed lncRNA target genes and mRNAs; D: KEGG pathway analysis of differentially expressed lncRNA target genes and mRNAs. lncRNA: Long noncoding RNA.

lymphangiogenesis[26]. However, our results indicate that BRAF^{V600E} mutation promotes angiogenesis and lymphoangiogenesis in the microenvironment.

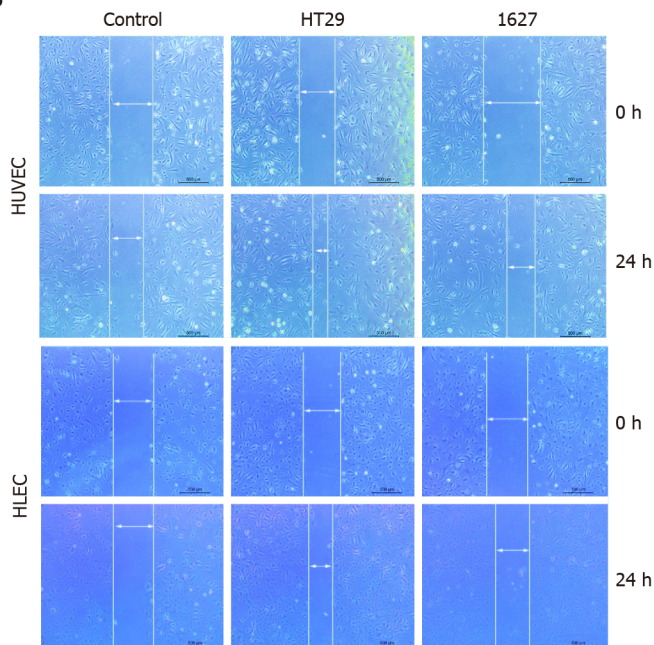
Simultaneously, BRAF^{V600E} mutation affected cellular components in the microenvironment. We identified that there was no difference in the content of CD68⁺ macrophages in BRAF^{V600E} mutant and BRAF wild-type CRC tissues, and the number of M2 macrophages was markedly higher than that of BRAF wild-type tissues. This is in agreement with the results reported in the literature. Compared with BRAF wild type tumor, there is no difference in CD68⁺ macrophages in BRAF^{V600E} mutant thyroid cancer, whereas M2 subtype macrophages increase[27]. Furthermore, TAMs have been positively related to lymph node and peritoneal metastasis in ovarian cancer, gastric cancer, and other tumors[28-30]. CAFs play an essential role in tumor development and metastasis. Our findings indicated no difference in the content of CAFs in CRC tissues of BRAF^{V600E} mutant and BRAF wild-type CRC. We hypothesized that BRAF^{V600E} mutant CRC might promote lymph node and peritoneal metastasis through other mechanisms, but the specific mechanism needs further exploration. This harsh microenvironment may lead to a worse prognosis and even result in resistance to traditional treatments.

Recent research has drawn a link between exosomes and intercellular communication, which are responsible for transporting specific RNA transcripts to target organs, participating in substance exchange in the distant environment, regulating immune function, and promoting tumor angiogenesis, invasion, and metastasis, thereby directly or indirectly affecting the progression and outcome of tumors[31]. We analyzed the expression profiles of exosomal lncRNAs and mRNAs in HT29 cells and 1627 cells using high-throughput sequencing, screening out differentially expressed lncRNAs and mRNAs. GO enrichment analysis and KEGG signaling pathway analysis were performed on differentially expressed lncRNA target genes and mRNAs. The findings indicated that differential lncRNA target genes were enriched in functions related to cell components, proliferation, metabolism, and migration, which were in agreement with functions of differential mRNA enrichment. The lncRNAs and mRNAs secreted by tumor cells were transported to target cells by exosomes. On the one hand, a microenvironment suitable for tumor cell metastasis (*i.e.*, premetastatic niche) could be created at a distance; on the other hand, it could also directly act on other tumor cells, altering their characteristics, and even change the metabolic programming of the tumor, thereby ultimately accelerating the invasion, metastasis,

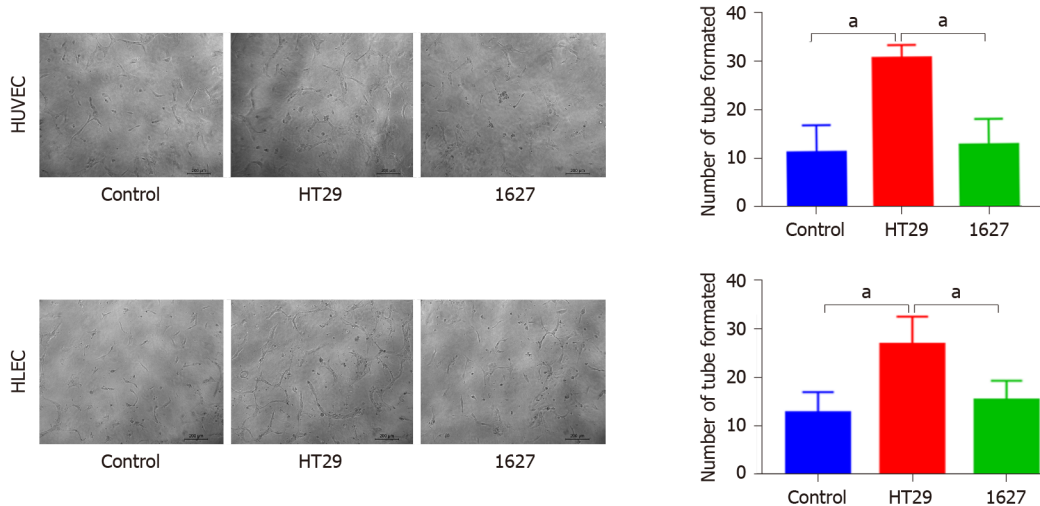
A



B



C



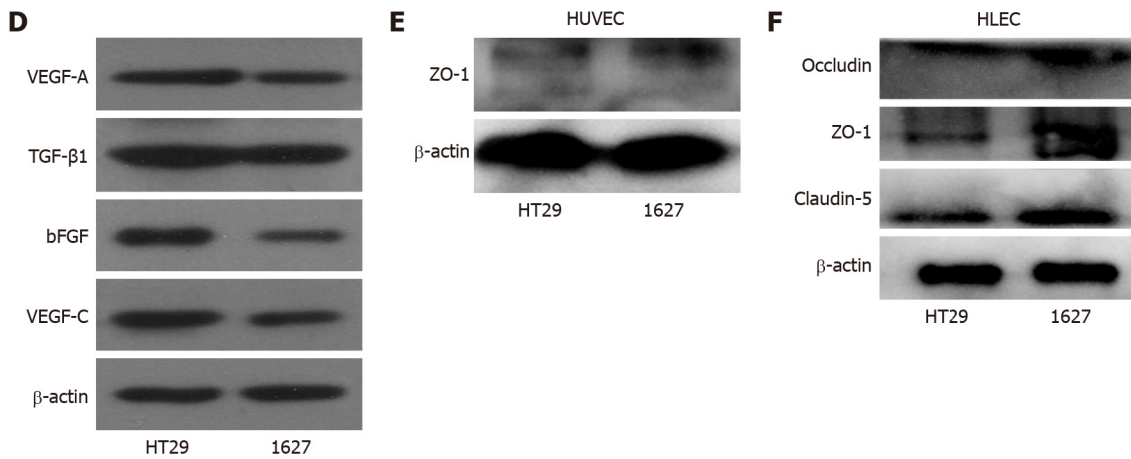


Figure 3 Effect of BRAF^{V600E} mutant colorectal cancer-cell-derived exosomes on the proliferation, migration, tube formation, and protein expression of human umbilical vein endothelial cells and human lymphatic endothelial cells. A: Detection of changes in proliferation of human umbilical vein endothelial cells (HUVECs) induced by exosomes derived from HT29 and 1627 cells at 24, 48, and 72 h by CCK8 assays. Changes in the proliferation of human lymphatic endothelial cells (HLECs) induced by exosomes derived from HT29 and 1627 cells were detected at 12, 24, and 36 h (the control group was treated with PBS); B: Detection of effects of HT29 and 1627 cell-derived exosomes on the migration of HUVECs and HLECs by scratch test ($\times 50$); C: After 24 h of incubation, the effect of HT29 and 1627 cell-derived exosomes on tube formation ability of HUVECs and HLECs was observed ($\times 100$); D: ELISA was used to detect expression of VEGF-A, TGF- β 1, bFGF, and VEGF-C proteins in exosomes derived from HT29 and 1627 cells; E: ELISA was used to detect the effect of exosomes derived from HT29 and 1627 cells on expression of ZO-1 proteins in HUVECs; F: ELISA was used to detect the effect of exosomes derived from HT29 and 1627 cells on expression of ZO-1, occludin, and claudin-5 proteins in HLECs. $^{\ast}P < 0.05$. HUVECs: Human umbilical vein endothelial cells; HLECs: Human lymphatic endothelial cells.

and drug resistance of tumors. The expression of the exosome-derived lncRNA RPPH1 in CRC was markedly upregulated and it simultaneously interacted with TAMs to promote the polarization of TAMs to M2 subtype, thereby accelerating tumor progression[21]. Gao *et al*[32] have found that the lncRNA 91H in tumor-cell-derived exosomes can increase the expression of heterogeneous nuclear ribonucleoprotein K, and markedly enhance the migration and invasion of CRC cells. The above evidence suggests that BRAF^{V600E} mutant CRC cells can reach the TME by releasing exosomal lncRNAs, and participate in tumor angiogenesis and tumor cell proliferation, differentiation, and metabolism through mRNAs, which are closely associated with the TME.

To explore the effect of exosomes secreted by BRAF^{V600E} mutant cells on the surrounding immune microenvironment, we cocultured exosomes derived from two colon cancer cell lines (HT29 and 1627) with HUVECs or HLECs. The exosomes derived from BRAF^{V600E} mutant CRC cells promoted proliferation, migration, and tube formation of endothelial cells, and induced angiogenesis and lymphoangiogenesis. Silencing BRAF gene generated corresponding inhibitory effects. BRAF^{V600E} mutation can promote the expression of matrix metalloproteinase-2 and VEGF-A in malignant melanoma cells, mediate angiogenesis, and enhance the invasiveness of tumor cells. However, BRAF gene deletion leads to a lack of VEGF-A, inhibiting angiogenesis and minimizing the permeability between endothelial cells[33]. Additional research has also proposed that BRAF^{V600E} mutant thyroid cancer cells can promote angiogenesis and lymphoangiogenesis by releasing VEGF-A and VEGF-C into the TME. Zelboraf can reduce the contents of these factors in the TME and inhibit angiogenesis and lymphoangiogenesis, thereby minimizing distant metastasis.

The expression of VEGF-A, bFGF, TGF- β , and VEGF-C proteins in exosomes derived from BRAF^{V600E} mutant CRC cells was also increased. Tight junction proteins ZO-1, claudin-5, and occludin participate in the formation of the endothelial barrier, affect cell permeability, and play a vital role in regulating the proliferation, migration, and tube formation of endothelial cells[34-36]. This study found that exosomes derived from BRAF^{V600E} mutant CRC cells could inhibit the expression of ZO-1, claudin-5, and occludin in HLECs and ZO-1 in HUVECs. Due to the low concentrations of claudin-5 and occludin in HUVECs, this study failed to detect the effect of silencing BRAF gene on the expression of claudin-5 and occludin proteins in HUVECs. Despite that inhibition of ZO-1, claudin-5, and occludin can restrain the growth of endothelial cells, it may not be enough to resist BRAF^{V600E} mutation for the promotion of vascularization (namely, increased expression of VEGF-A, bFGF, TGF- β , and VEGF-C proteins). Our study suggests that exosomes derived from BRAF^{V600E} mutant CRC cells promote the expression of VEGF-A, bFGF, TGF- β , and VEGF-C to facilitate

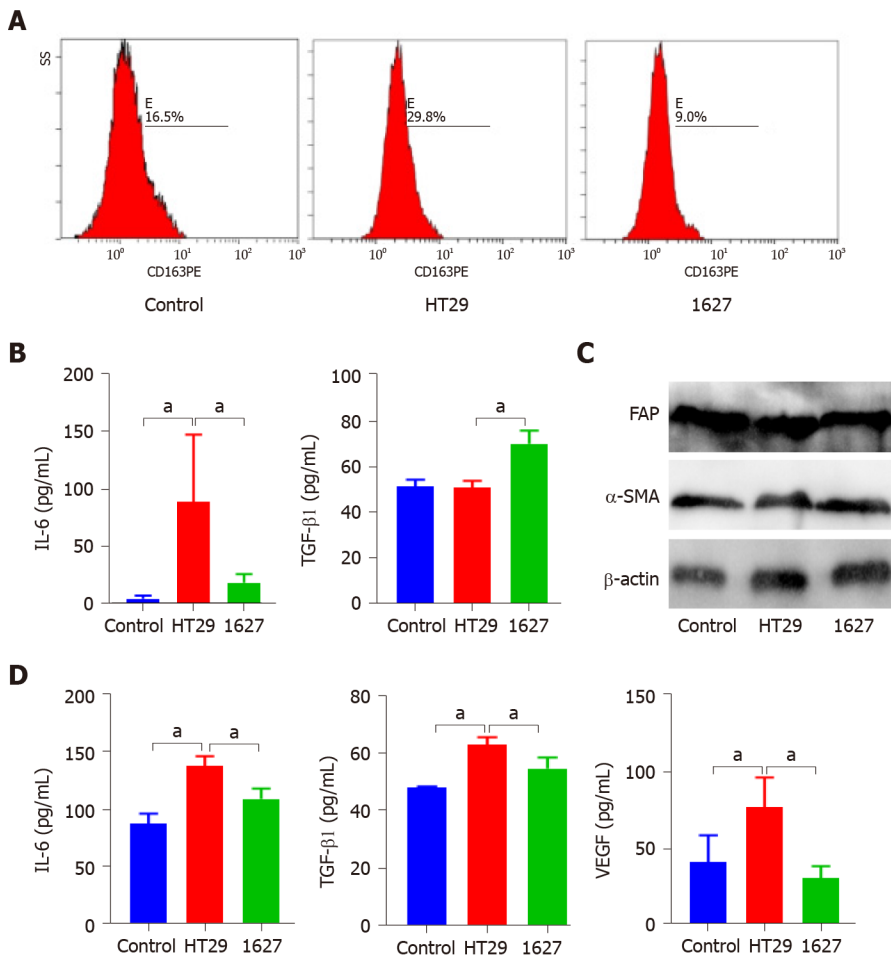


Figure 4 Effect of exosomes derived from BRAF^{V600E} mutant colorectal cancer cells on the phenotype and secretion function of tumor-associated macrophages and cancer-associated fibroblasts. A: Effect of silencing BRAF gene on expression of CD163 in macrophages induced by exosomes derived from BRAF^{V600E} mutant colorectal cancer cells; B: ELISA was used to detect expression of interleukin (IL)-6 and transforming growth factor (TGF)-β1 in the supernatant of THP-1 cells; C: Western blotting was used to detect expression of FAP and α-SMA in MRC-5 cells; D: ELISA was used to detect expression of IL-6, TGF-β1, and vascular endothelial growth factor in the supernatant of MRC-5 cells. ^a*P* < 0.05. VEGF: Vascular endothelial growth factor; IL: Interleukin; TGF: Transforming growth factor.

angiogenesis and lymphangiogenesis.

We cocultured exosomes derived from HT29 and 1627 cells with macrophages and found that exosomes derived from BRAF^{V600E} mutant CRC cells enhanced the polarization of macrophages to M2 subtype. M1 subtype macrophages secrete IL-6, and M2 subtype macrophages secrete TGF-β1[37]. IL-6 is highly expressed in diverse malignant TMEs, and it can promote tumor invasion, distant metastasis, and angiogenesis, and participate in tumor resistance[38]. Exosomes derived from BRAF^{V600E} mutant colon cancer cells can promote the secretion of IL-6 by macrophages and after silencing the BRAF gene, exosomes can inhibit the secretion of IL-6 by macrophages. Some researchers have discovered that exosomes secreted by hepatoma promote the secretion of IL-6 by macrophages, whereas exosomes secreted by melatonin-treated hepatocellular carcinoma can inhibit the secretion of IL-6 by macrophages[39]. TGF-β1 inhibits tumor proliferation and induces apoptosis in the early stage of tumor development. Conversely, when in the advanced stage, it promotes the development and metastasis of the tumor by promoting epithelial-mesenchymal transition, regulating the microenvironment and the immune system[40,41]. Some studies have found that BRAF^{V600E} mutant CRC-derived exosomes can inhibit macrophages from secreting more TGF-β1. Therefore, we speculated that exosomes derived from BRAF^{V600E} mutant CRC cells could promote the polarization of macrophages to M2 subtype, increase the secretion of IL-6, and reduce the secretion of TGF-β1, thereby facilitating distant metastasis.

The cell component with the highest content in the microenvironment is CAFs, which highly express α-SMA and FAP, and secrete IL-6, TGF-β1, and VEGF. Meanwhile, they assist tumor cells in immune escape, and promote angiogenesis,

tumor invasion, and metastasis[42,43]. The present study indicated that after exosomes derived from BRAF^{V600E} mutant CRC cells were cocultured with fibroblasts, the expression of α -SMA and FAP in fibroblasts did not change markedly. Instead, they promoted the secretion of IL-6 and TGF- β 1 and VEGF by CAFs. It was suggested that BRAF^{V600E} mutation had little effect on the number of CAFs, mainly affecting their function. Some researchers have found that exosomes derived from hepatocellular carcinoma can promote the differentiation of hepatic astrocytes into CAFs. The activated CAFs secrete cytokines VEGF, TGF- β , and IL-6, and promote angiogenesis and liver metastasis[44,45].

We selected only one BRAF^{V600E} mutant CRC cell line, and only performed *in vitro* experiments. The differentially expressed lncRNAs were not verified. Nevertheless, our research demonstrated that BRAF^{V600E} mutant CRC had a unique immune microenvironment, which might be induced by the release of exosomes rich in certain lncRNAs. Therefore, in the future, we can consider to reshape the immune microenvironment, combined with traditional treatment, to treat this specific type of CRC.

CONCLUSION

Our study showed that, compared with wild type BRAF, BRAF^{V600E} mutation led to more angiogenesis and lymphoangiogenesis in the microenvironment. Meanwhile, the polarization of macrophages to M2 subtype was more obvious, and the immunosuppression was more prominent. Further analysis indicated that exosomes derived from BRAF^{V600E} mutant CRC cells were rich in certain lncRNAs and mRNAs, which might be linked to these alterations. This provides a hypothesis for finding new therapeutic strategies for BRAF^{V600E} mutant CRC.

ARTICLE HIGHLIGHTS

Research background

BRAF^{V600E} gene mutation accounts for approximately 10% of patients with metastatic colorectal cancer (CRC). Compared with CRC patients with wild-type BRAF, patients with BRAF^{V600E} mutant CRC are prone to peritoneal metastasis and distant lymph node metastasis with a poor prognosis. Previous findings suggest that BRAF^{V600E} mutation affects the tumor microenvironment (TME).

Research motivation

BRAF^{V600E} mutation is involved in the formation of the immunosuppressive microenvironment in thyroid cancer. However, the influence and the related mechanism of BRAF^{V600E} mutation in CRC on the surrounding immune microenvironment are not clear.

Research objectives

The study aimed to determine the influence of BRAF^{V600E} mutation in CRC on the surrounding immune microenvironment, elucidating whether BRAF^{V600E} mutant CRC cell-derived exosomes participate in the formation of an immunosuppressive microenvironment.

Research methods

CRC patients were divided into either a control group or a treatment group. The formation of microvessels and microlymphatic vessels and M2 subtype macrophages in tumor tissues were detected by immunohistochemistry. Screening and functional analysis of exosomal long noncoding RNAs (lncRNAs) were performed by transcriptomics. The proliferation and migration of human umbilical vein endothelial cells (HUVECs) and human lymphatic endothelial cells (HLECs) were detected by CCK-8 assays and scratch test, respectively. The tube-forming ability of endothelial cells was assessed by tube formation assay. The macrophage subtypes were obtained by flow cytometry. The expression of vascular endothelial growth factor (VEGF)-A, basic fibroblast growth factor (bFGF), transforming growth factor (TGF)- β 1, VEGF-C, claudin-5, occludin, zonula occludens (ZO)-1, fibroblast activation protein (FAP), and α -smooth muscle actin was assessed by Western blot analysis. The levels of cytokines interleukin (IL)-6, TGF- β 1, and VEGF were assessed by ELISA.

Research results

BRAF^{V600E} mutation was positively correlated with a poor prognosis in CRC ($P < 0.01$). Microvascular density and microlymphatic vessel density in BRAF^{V600E} mutant CRC tissues were higher than those in BRAF wild-type CRC ($P < 0.05$). The number of CD163⁺ M2 macrophages in BRAF^{V600E} mutant CRC tumor tissue was markedly increased ($P < 0.05$). Compared with exosomes from CRC cells with BRAF gene silencing, the expression of 13 lncRNAs and 192 mRNAs in the BRAF^{V600E} mutant CRC cell exosomes was upregulated, and the expression of 22 lncRNAs and 236 mRNAs was downregulated ($P < 0.05$). The biological functions and signaling pathways predicted by differential lncRNA target genes and differential mRNA were closely related to angiogenesis, tumor cell proliferation, differentiation, metabolism, and changes in the microenvironment. The proliferation, migration, and tube formation ability of HUVECs and HLECs induced by exosomes in the 1627 cell group (HT29 cells with BRAF gene silencing) was greatly reduced compared with the HT29 cell group ($P < 0.05$). Compared with the HT29 cell group, the expression levels of VEGF-A, bFGF, TGF- β 1, and VEGF-C in the exosomes derived from 1627 cells were reduced. The expression of ZO-1 in HUVECs, and claudin-5, occludin, and ZO-1 in HLECs of the 1627 cell group was higher. Compared with the 1627 cell group, the exosomes of the HT29 group promoted the expression of CD163 in macrophages ($P < 0.05$). IL-6 secretion by macrophages in the HT29 cell group was markedly elevated ($P < 0.05$), whereas TGF- β 1 was decreased ($P < 0.05$). The levels of IL-6, TGF- β 1, and VEGF secreted by fibroblasts in the 1627 cell group decreased, compared with the HT29 group ($P < 0.05$).

Research conclusions

BRAF^{V600E} mutant CRC cells can reach the TME by releasing exosomal lncRNAs, inducing the formation of an immunosuppressive microenvironment.

Research perspectives

The study will provide a novel therapeutic strategy for BRAF^{V600E} mutant CRC.

REFERENCES

- 1 Siegel RL, Miller KD, Jemal A. Cancer statistics, 2019. *CA Cancer J Clin* 2019; **69**: 7-34 [PMID: 30620402 DOI: 10.3322/caac.21551]
- 2 Zhou J, Zheng R, Zhang S, Zeng H, Wang S, Chen R, Sun K, Li M, Gu J, Zhuang G, Wei W. Colorectal cancer burden and trends: Comparison between China and major burden countries in the world. *Chin J Cancer Res* 2021; **33**: 1-10 [PMID: 33707923 DOI: 10.21147/j.issn.1000-9604.2021.01.01]
- 3 Fiskus W, Mitsiades N. B-Raf Inhibition in the Clinic: Present and Future. *Annu Rev Med* 2016; **67**: 29-43 [PMID: 26768236 DOI: 10.1146/annurev-med-090514-030732]
- 4 Ursem C, Atreya CE, Van Loon K. Emerging treatment options for BRAF-mutant colorectal cancer. *Gastrointest Cancer* 2018; **8**: 13-23 [PMID: 29628780 DOI: 10.2147/GICTT.S125940]
- 5 Taieb J, Lapeyre-Prost A, Laurent Puig P, Zaanani A. Exploring the best treatment options for BRAF-mutant metastatic colon cancer. *Br J Cancer* 2019; **121**: 434-442 [PMID: 31353365 DOI: 10.1038/s41416-019-0526-2]
- 6 Davies H, Bignell GR, Cox C, Stephens P, Edkins S, Clegg S, Teague J, Woffendin H, Garnett MJ, Bottomley W, Davis N, Dicks E, Ewing R, Floyd Y, Gray K, Hall S, Hawes R, Hughes J, Kosmidou V, Menzies A, Mould C, Parker A, Stevens C, Watt S, Hooper S, Wilson R, Jayatilake H, Gusterson BA, Cooper C, Shipley J, Hargrave D, Pritchard-Jones K, Maitland N, Chenevix-Trench G, Riggins GJ, Bigner DD, Palmieri G, Cossu A, Flanagan A, Nicholson A, Ho JW, Leung SY, Yuen ST, Weber BL, Seigler HF, Darrow TL, Paterson H, Marais R, Marshall CJ, Wooster R, Stratton MR, Futreal PA. Mutations of the BRAF gene in human cancer. *Nature* 2002; **417**: 949-954 [PMID: 12068308 DOI: 10.1038/nature00766]
- 7 Fedorenko IV, Paraiso KH, Smalley KS. Acquired and intrinsic BRAF inhibitor resistance in BRAF V600E mutant melanoma. *Biochem Pharmacol* 2011; **82**: 201-209 [PMID: 21635872 DOI: 10.1016/j.bcp.2011.05.015]
- 8 Bhatt KV, Spofford LS, Aram G, McMullen M, Pumiglia K, Aplin AE. Adhesion control of cyclin D1 and p27Kip1 Levels is deregulated in melanoma cells through BRAF-MEK-ERK signaling. *Oncogene* 2005; **24**: 3459-3471 [PMID: 15735667 DOI: 10.1038/sj.onc.1208544]
- 9 Jin Z, Sinicrope FA. Advances in the therapy of BRAF^{V600E} metastatic colorectal cancer. *Expert Rev Anticancer Ther* 2019; **19**: 823-829 [PMID: 31455117 DOI: 10.1080/14737140.2019.1661778]
- 10 Biller LH, Schrag D. Diagnosis and Treatment of Metastatic Colorectal Cancer: A Review. *JAMA* 2021; **325**: 669-685 [PMID: 33591350 DOI: 10.1001/jama.2021.0106]
- 11 Wong V, Lee M, Wong R, Tie J, Shapiro J, Desai J, Nott L, Steel S, Burge M, Ma B, Khattak A,

- Hong W, Gibbs P. BRAFV600E Mutations Arising from a Left-Side Primary in Metastatic Colorectal Cancer: Are They a Distinct Subset? *Target Oncol* 2021; **16**: 227-236 [PMID: 33599905 DOI: 10.1007/s11523-021-00793-7]
- 12 **Galon J**, Bruni D. Tumor Immunology and Tumor Evolution: Intertwined Histories. *Immunity* 2020; **52**: 55-81 [PMID: 31940273 DOI: 10.1016/j.immuni.2019.12.018]
 - 13 **Means C**, Clayburgh DR, Maloney L, Sauer D, Taylor MH, Shindo ML, Coussens LM, Tsujikawa T. Tumor immune microenvironment characteristics of papillary thyroid carcinoma are associated with histopathological aggressiveness and BRAF mutation status. *Head Neck* 2019; **41**: 2636-2646 [PMID: 30896061 DOI: 10.1002/hed.25740]
 - 14 **Denton AE**, Roberts EW, Fearon DT. Stromal Cells in the Tumor Microenvironment. *Adv Exp Med Biol* 2018; **1060**: 99-114 [PMID: 30155624 DOI: 10.1007/978-3-319-78127-3_6]
 - 15 **Erreni M**, Mantovani A, Allavena P. Tumor-associated Macrophages (TAM) and Inflammation in Colorectal Cancer. *Cancer Microenviron* 2011; **4**: 141-154 [PMID: 21909876 DOI: 10.1007/s12307-010-0052-5]
 - 16 **Herrera M**, Herrera A, Domínguez G, Silva J, García V, García JM, Gómez I, Soldevilla B, Muñoz C, Provencio M, Campos-Martin Y, García de Herrerros A, Casal I, Bonilla F, Peña C. Cancer-associated fibroblast and M2 macrophage markers together predict outcome in colorectal cancer patients. *Cancer Sci* 2013; **104**: 437-444 [PMID: 23298232 DOI: 10.1111/cas.12096]
 - 17 **Ping Q**, Yan R, Cheng X, Wang W, Zhong Y, Hou Z, Shi Y, Wang C, Li R. Cancer-associated fibroblasts: overview, progress, challenges, and directions. *Cancer Gene Ther* 2021; **28**: 984-999 [PMID: 33712707 DOI: 10.1038/s41417-021-00318-4]
 - 18 **Bracci L**, Lozupone F, Parolini I. The role of exosomes in colorectal cancer disease progression and response to therapy. *Cytokine Growth Factor Rev* 2020; **51**: 84-91 [PMID: 31955973 DOI: 10.1016/j.cytogfr.2019.12.004]
 - 19 **Galamb O**, Barták BK, Kalmár A, Nagy ZB, Szigeti KA, Tulassay Z, Igaz P, Molnár B. Diagnostic and prognostic potential of tissue and circulating long non-coding RNAs in colorectal tumors. *World J Gastroenterol* 2019; **25**: 5026-5048 [PMID: 31558855 DOI: 10.3748/wjg.v25.i34.5026]
 - 20 **Sun Z**, Liu J, Chen C, Zhou Q, Yang S, Wang G, Song J, Li Z, Zhang Z, Xu J, Sun X, Chang Y, Yuan W. The Biological Effect and Clinical Application of Long Noncoding RNAs in Colorectal Cancer. *Cell Physiol Biochem* 2018; **46**: 431-441 [PMID: 29614491 DOI: 10.1159/000488610]
 - 21 **Liang ZX**, Liu HS, Wang FW, Xiong L, Zhou C, Hu T, He XW, Wu XJ, Xie D, Wu XR, Lan P. LncRNA RPPH1 promotes colorectal cancer metastasis by interacting with TUBB3 and by promoting exosomes-mediated macrophage M2 polarization. *Cell Death Dis* 2019; **10**: 829 [PMID: 31685807 DOI: 10.1038/s41419-019-2077-0]
 - 22 **Wang J**, Shen J, Huang C, Cao M, Shen L. Clinicopathological Significance of BRAFV600E Mutation in Colorectal Cancer: An Updated Meta-Analysis. *J Cancer* 2019; **10**: 2332-2341 [PMID: 31258736 DOI: 10.7150/jca.30789]
 - 23 **Caputo F**, Santini C, Bardasi C, Cerma K, Casadei-Gardini A, Spallanzani A, Andrikou K, Cascinu S, Gelsomino F. BRAF-Mutated Colorectal Cancer: Clinical and Molecular Insights. *Int J Mol Sci* 2019; **20** [PMID: 31661924 DOI: 10.3390/ijms20215369]
 - 24 **Husain A**, Hu N, Sadow PM, Nucera C. Expression of angiogenic switch, cachexia and inflammation factors at the crossroad in undifferentiated thyroid carcinoma with BRAF(V600E). *Cancer Lett* 2016; **380**: 577-585 [PMID: 26189429 DOI: 10.1016/j.canlet.2015.07.012]
 - 25 **Hu HY**, Yu CH, Zhang HH, Zhang SZ, Yu WY, Yang Y, Chen Q. Exosomal miR-1229 derived from colorectal cancer cells promotes angiogenesis by targeting HIPK2. *Int J Biol Macromol* 2019; **132**: 470-477 [PMID: 30936013 DOI: 10.1016/j.ijbiomac.2019.03.221]
 - 26 **Sun B**, Zhou Y, Fang Y, Li Z, Gu X, Xiang J. Colorectal cancer exosomes induce lymphatic network remodeling in lymph nodes. *Int J Cancer* 2019; **145**: 1648-1659 [PMID: 30734278 DOI: 10.1002/ijc.32196]
 - 27 **Angell TE**, Lechner MG, Jang JK, Correa AJ, LoPresti JS, Epstein AL. BRAF V600E in papillary thyroid carcinoma is associated with increased programmed death ligand 1 expression and suppressive immune cell infiltration. *Thyroid* 2014; **24**: 1385-1393 [PMID: 24955518 DOI: 10.1089/thy.2014.0134]
 - 28 **Wang R**, Zhang T, Ma Z, Wang Y, Cheng Z, Xu H, Li W, Wang X. The interaction of coagulation factor XII and monocyte/macrophages mediating peritoneal metastasis of epithelial ovarian cancer. *Gynecol Oncol* 2010; **117**: 460-466 [PMID: 20233624 DOI: 10.1016/j.ygyno.2010.02.015]
 - 29 **Yamagata Y**, Tomioka H, Sakamoto K, Sato K, Harada H, Ikeda T, Kayamori K. CD163-Positive Macrophages Within the Tumor Stroma Are Associated With Lymphangiogenesis and Lymph Node Metastasis in Oral Squamous Cell Carcinoma. *J Oral Maxillofac Surg* 2017; **75**: 2144-2153 [PMID: 28399391 DOI: 10.1016/j.joms.2017.03.009]
 - 30 **Go Y**, Tanaka H, Tokumoto M, Sakurai K, Toyokawa T, Kubo N, Muguruma K, Maeda K, Ohira M, Hirakawa K. Tumor-Associated Macrophages Extend Along Lymphatic Flow in the Pre-metastatic Lymph Nodes of Human Gastric Cancer. *Ann Surg Oncol* 2016; **23** Suppl 2: S230-S235 [PMID: 25743331 DOI: 10.1245/s10434-015-4458-7]
 - 31 **Kok VC**, Yu CC. Cancer-Derived Exosomes: Their Role in Cancer Biology and Biomarker Development. *Int J Nanomedicine* 2020; **15**: 8019-8036 [PMID: 33116515 DOI: 10.2147/IJN.S272378]
 - 32 **Gao T**, Liu X, He B, Nie Z, Zhu C, Zhang P, Wang S. Exosomal lncRNA 91H is associated with poor development in colorectal cancer by modifying HNRNPK expression. *Cancer Cell Int* 2018; **18**: 11

- [PMID: 29410604 DOI: 10.1186/s12935-018-0506-2]
- 33 **Declercq M**, Treps L. BRAF, A gatekeeper controlling endothelial permeability. *FEBS J* 2019; **286**: 2273-2276 [PMID: 31081213 DOI: 10.1111/febs.14861]
 - 34 **Tornavaca O**, Chia M, Dufton N, Almagro LO, Conway DE, Randi AM, Schwartz MA, Matter K, Balda MS. ZO-1 controls endothelial adherens junctions, cell-cell tension, angiogenesis, and barrier formation. *J Cell Biol* 2015; **208**: 821-838 [PMID: 25753039 DOI: 10.1083/jcb.201404140]
 - 35 **Chidiac R**, Zhang Y, Tessier S, Faubert D, Delisle C, Gratton JP. Comparative Phosphoproteomics Analysis of VEGF and Angiopoietin-1 Signaling Reveals ZO-1 as a Critical Regulator of Endothelial Cell Proliferation. *Mol Cell Proteomics* 2016; **15**: 1511-1525 [PMID: 26846344 DOI: 10.1074/mcp.M115.053298]
 - 36 **Zhang H**, Zhang S, Zhang J, Liu D, Wei J, Fang W, Zhao W, Chen Y, Shang D. ZO-1 expression is suppressed by GM-CSF via miR-96/ERG in brain microvascular endothelial cells. *J Cereb Blood Flow Metab* 2018; **38**: 809-822 [PMID: 28430012 DOI: 10.1177/0271678X17702668]
 - 37 **Xu YW**, Xing RX, Zhang WH, Li L, Wu Y, Hu J, Wang C, Luo QL, Shen JL, Chen X. *Toxoplasma* ROP16_{tm} ameliorated inflammatory bowel diseases via inducing M2 phenotype of macrophages. *World J Gastroenterol* 2019; **25**: 6634-6652 [PMID: 31832003 DOI: 10.3748/wjg.v25.i45.6634]
 - 38 **Choy EH**, De Benedetti F, Takeuchi T, Hashizume M, John MR, Kishimoto T. Translating IL-6 biology into effective treatments. *Nat Rev Rheumatol* 2020; **16**: 335-345 [PMID: 32327746 DOI: 10.1038/s41584-020-0419-z]
 - 39 **Cheng L**, Liu J, Liu Q, Liu Y, Fan L, Wang F, Yu H, Li Y, Bu L, Li X, Wei W, Wang H, Sun G. Exosomes from Melatonin Treated Hepatocellularcarcinoma Cells Alter the Immunosuppression Status through STAT3 Pathway in Macrophages. *Int J Biol Sci* 2017; **13**: 723-734 [PMID: 28655998 DOI: 10.7150/ijbs.19642]
 - 40 **Liu S**, Ren J, Ten Dijke P. Targeting TGFβ signal transduction for cancer therapy. *Signal Transduct Target Ther* 2021; **6**: 8 [PMID: 33414388 DOI: 10.1038/s41392-020-00436-9]
 - 41 **Derynck R**, Turley SJ, Akhurst RJ. TGFβ biology in cancer progression and immunotherapy. *Nat Rev Clin Oncol* 2021; **18**: 9-34 [PMID: 32710082 DOI: 10.1038/s41571-020-0403-1]
 - 42 **Piersma B**, Hayward MK, Weaver VM. Fibrosis and cancer: A strained relationship. *Biochim Biophys Acta Rev Cancer* 2020; **1873**: 188356 [PMID: 32147542 DOI: 10.1016/j.bbcan.2020.188356]
 - 43 **Lim H**, Koh M, Jin H, Bae M, Lee SY, Kim KM, Jung J, Kim HJ, Park SY, Kim HS, Moon WK, Hwang S, Cho NH, Moon A. Cancer-associated fibroblasts induce an aggressive phenotypic shift in non-malignant breast epithelial cells via interleukin-8 and S100A8. *J Cell Physiol* 2021; **236**: 7014-7032 [PMID: 33748944 DOI: 10.1002/jcp.30364]
 - 44 **Zhou Y**, Ren H, Dai B, Li J, Shang L, Huang J, Shi X. Hepatocellular carcinoma-derived exosomal miRNA-21 contributes to tumor progression by converting hepatocyte stellate cells to cancer-associated fibroblasts. *J Exp Clin Cancer Res* 2018; **37**: 324 [PMID: 30591064 DOI: 10.1186/s13046-018-0965-2]
 - 45 **Fang T**, Lv H, Lv G, Li T, Wang C, Han Q, Yu L, Su B, Guo L, Huang S, Cao D, Tang L, Tang S, Wu M, Yang W, Wang H. Tumor-derived exosomal miR-1247-3p induces cancer-associated fibroblast activation to foster lung metastasis of liver cancer. *Nat Commun* 2018; **9**: 191 [PMID: 29335551 DOI: 10.1038/s41467-017-02583-0]



Published by **Baishideng Publishing Group Inc**
7041 Koll Center Parkway, Suite 160, Pleasanton, CA 94566, USA

Telephone: +1-925-3991568

E-mail: bpgoffice@wjgnet.com

Help Desk: <https://www.f6publishing.com/helpdesk>

<https://www.wjgnet.com>

